



Research article

An approximation method for convolution curves of regular curves and ellipses

Young Joon Ahn*

Department of Mathematics Education, Chosun University, Gwangju 61452, South Korea

* **Correspondence:** Email: ahn@chosun.ac.kr.

Abstract: In this paper, we present a method of G^2 Hermite interpolation of convolution curves of regular plane curves and ellipses. We show that our approximant is also a C^1 Hermite interpolation of the convolution curve. This method yields a polynomial curve if the trajectory curve is a polynomial curve. Our approximation method is applied to two previous numerical examples. The results of our method are compared with those of previous methods, and the merits and demerits are analyzed. Compared with previous methods, the merits of our method are that the approximant is G^2 and C^1 Hermite interpolation, and the degree of the approximant or the required number of segments of the approximant within error tolerances is small.

Keywords: convolution approximation; Hermite interpolation; polynomial curve; Hausdorff distance; signed curvature continuity

Mathematics Subject Classification: 41A05, 65D17

1. Introduction

Minkowski sum has been used in various important geometric computations, for example, for collision detection between objects [1, 2] and computing collision-free paths in robot motion planning [3–5]. The convolution curves of two plane curves are related to the Minkowski sum boundaries in the plane. The Minkowski sum boundaries of two plane objects is a subset of the convolution curves of the boundaries of the objects [1, 6, 7].

Convolution curves and surfaces have been studied extensively in the literature. The results for classical offsets on convolutions of algebraic curves have been generalized, and a closed formula expressing the convolution degree by means of the algebraic degree and genus of the curve, has been derived [6]. Additionally, the class of rational hypersurfaces which have the same convolution properties as hyperspheres has been identified, and their geometric and algebraic properties have been investigated [7]. The Hausdorff distance between two regular plane curves has been

shown to be invariant under convolution with the same regular curve provided the curves have no cusp [8]. Convolution curves at endpoints are characterized with respect to the tangent and bending directions [9].

In general, the convolution curves of two polynomial or rational curves are neither polynomial nor rational curves. Thus, it is necessary to approximate the convolution curves of two polynomial or rational curves by polynomial or rational curves. The convolution curve of a quadratic curve and other polynomial curves is rational, and using this property, one of the two polynomial curves is approximated by a quadratic curve, and so their convolution curve can be approximated by the rational curve [1]. This property can be applied to offset approximation [10, 11]. If two curves have the parallel derivative, then their convolution curve is obtained easily by their simple addition [12]. Using this property, the convolution of two curves is approximated by cubic curves after the two curves are approximated by two cubic curves with the parallel derivatives [12]. The linear normal surfaces have rational offsets [13, 14]. The convolution surface of a linear normal surface and other rational surfaces is rational [15, 16], and the same property holds for the curve case. Using this property, the approximation of convolution curves of ellipses and general polynomial curves can be presented based on the ellipse approximation by linear normal curves [17].

In this paper, we present an approximation method for the convolution curve of an ellipse and a regular trajectory curve. We obtain the sufficient condition for the existence of at least a G^0 approximant of the convolution curve using our method. In addition, we characterize the necessary and sufficient condition for the G^0 approximant to be a G^2 approximation of the convolution curve. Moreover, we show that the G^2 Hermite interpolation is also a C^1 interpolation of the convolution curve. In our method, if the trajectory curve is the polynomial curve, then so is our approximant. We apply our method to previous examples in the literature. We implement our method and previous methods, and compare and analyze their results.

The remainder of this paper is organized as follows: In Section 2, the known properties of the convolution of two compatible parametric curves are introduced. In Section 3, our approximation method for the convolution curves of trajectory curves and ellipses is presented. We apply our method to existing examples in Section 4 and summarize our work in Section 5.

2. Preliminaries

In this section, we present the preliminaries and notions related to convolution curves of regular plane curves [1, 8, 10]. Let $\mathbf{x}_i : [a_i, b_i] \rightarrow \mathbb{R}^2$, $i = 1, 2$, be two regular plane curves. They are said to be compatible [1, 9], if there exists a reparametrization $s = s(t)$ satisfying $\mathbf{x}'_1(t) \parallel \mathbf{x}'_2(s(t))$. The convolution curve $\mathbf{x}_1 * \mathbf{x}_2$ for two compatible curves $\mathbf{x}_1, \mathbf{x}_2$ is defined by

$$(\mathbf{x}_1 * \mathbf{x}_2)(t) = \mathbf{x}_1(t) + \mathbf{x}_2(s(t)).$$

The reparameterized curve $\mathbf{x}_2(s(t))$ is denoted by $\tilde{\mathbf{x}}_2(t)$, i.e., $\tilde{\mathbf{x}}_2(t) = \mathbf{x}_2(s(t))$. Let $\kappa_{\mathbf{x}}(t)$ be the (signed) curvature of the plane curve \mathbf{x} at the point $\mathbf{x}(t)$. The curvature of $\mathbf{x}_1 * \tilde{\mathbf{x}}_2$ is

$$\kappa_{\mathbf{x}_1 * \tilde{\mathbf{x}}_2} = \text{sign}(\kappa_{\mathbf{x}_1}) \frac{\kappa_{\mathbf{x}_1} \kappa_{\tilde{\mathbf{x}}_2}}{|\kappa_{\mathbf{x}_1} \pm \kappa_{\tilde{\mathbf{x}}_2}|} = \text{sign}(\kappa_{\mathbf{x}_1}) \left| \frac{\kappa_{\mathbf{x}_1} \kappa_{\tilde{\mathbf{x}}_2}}{|\kappa_{\mathbf{x}_1}| \pm |\kappa_{\tilde{\mathbf{x}}_2}|} \right|, \quad (2.1)$$

where we choose the + sign when \mathbf{x}_1 and $\tilde{\mathbf{x}}_2$ are parallel and the – sign when they are anti-parallel [18]. Note that if either $\kappa_{\mathbf{x}_1}$ or $\kappa_{\tilde{\mathbf{x}}_2}$ is zero, then $\kappa_{\mathbf{x}_1 * \tilde{\mathbf{x}}_2}$ is also zero. In general, the sign of the curvature of \mathbf{x}_1 is

the same as that of $\tilde{\mathbf{x}}_2$. Note that

$$\kappa_{\tilde{\mathbf{x}}_2}(t)\tilde{\mathbf{x}}_2'(t) = \pm\kappa_{\mathbf{x}_1}(t)\mathbf{x}_1'(t), \quad (2.2)$$

where, likewise, the + sign holds when \mathbf{x}_1 and $\tilde{\mathbf{x}}_2$ are parallel, and the – sign holds when they are anti-parallel.

The Hausdorff distance is invariant under convolution, i.e., for a regular plane curve \mathbf{x} ,

$$d_H(\mathbf{x}_1 * \mathbf{x}, \mathbf{x}_2 * \mathbf{x}) = d_H(\mathbf{x}_1, \mathbf{x}_2), \quad (2.3)$$

if these curves are regular [8].

3. G^2 Hermite interpolation of convolution curve of trajectory curve and ellipse

In this section, we present an approximation method for G^2 and C^1 Hermite interpolation of convolution curves of regular plane curves and ellipses.

Let $\mathbf{x} : [0, 1] \rightarrow \mathbb{R}^2$ be a regular parametric plane curve. Let $\mathbf{e} : \mathbb{R} \rightarrow \mathbb{R}^2$ be an ellipse centered at the origin whose long and short radii are a and b . The region generated by moving the ellipse along the trajectory curve \mathbf{x} is the Minkowski sum of \mathbf{x} and \mathbf{e} , and its boundary can be obtained by the convolution curve of \mathbf{x} and \mathbf{e} . The ellipse \mathbf{e} has two sided curve segments which are compatible to \mathbf{x} , i.e., there are reparametrizations s_+ and s_- such that

$$\mathbf{x}'(t) \parallel \mathbf{e}'(s_+(t)) \parallel \mathbf{e}'(s_-(t)), \quad \pm\mathbf{x}'(t) \times \mathbf{e}(s_{\pm}(t)) < 0.$$

Let two curves $\mathbf{e}_+, \mathbf{e}_- : [0, 1] \rightarrow \mathbb{R}^2$ be defined by the reparameterization $\mathbf{e}_{\pm}(t) = \mathbf{e}(s_{\pm}(t))$. Two convolution curves of \mathbf{x} and \mathbf{e} are obtained by

$$\mathbf{x} * \mathbf{e}_+(t) = \mathbf{x}(t) + \mathbf{e}_+(t), \quad \mathbf{x} * \mathbf{e}_-(t) = \mathbf{x}(t) + \mathbf{e}_-(t).$$

In general, \mathbf{e}_{\pm} cannot be expressed by rational curves even if \mathbf{x} is a polynomial curve. Thus, approximations for \mathbf{e}_{\pm} are needed. Let $\mathbf{e}_{\pm}^a : [0, 1] \rightarrow \mathbb{R}^2$ be our approximants for \mathbf{e}_{\pm} , respectively. Our approximants are proposed as in (3.1), so that $\mathbf{e}_{\pm}^{a'}(t)$ and $\mathbf{x}'(t)$ are parallel for $t \in [0, 1]$, and then their convolution can be directly obtained by their simple addition, i.e.,

$$\mathbf{x} * \mathbf{e}_+^a(t) = \mathbf{x}(t) + \mathbf{e}_+^a(t), \quad \mathbf{x} * \mathbf{e}_-^a(t) = \mathbf{x}(t) + \mathbf{e}_-^a(t).$$

This idea was originally presented in [12], and later used in [19, 20]. We propose the approximants

$$\mathbf{e}_{\pm}^a(t) = \int_0^t \mathbf{x}'(u)\alpha(u)du + \mathbf{e}_{\pm}(0), \quad (3.1)$$

where $\alpha : [0, 1] \rightarrow \mathbb{R}$ is a cubic polynomial defined by

$$\alpha(t) = \sum_{i=0}^3 \alpha_i B_i^3(t),$$

and $B_i^n(t) = \binom{n}{i} t^i (1-t)^{n-i}$, $0 \leq i \leq n$, are the Bernstein polynomials of degree n . Note that since \mathbf{e}_- is equal to $-\mathbf{e}_+$, we can obtain \mathbf{e}_-^a by $-\mathbf{e}_+^a$. If \mathbf{e}_+^a is a G^2 interpolation of \mathbf{e}_+ , then \mathbf{e}_-^a is also a G^2 interpolation

of \mathbf{e}_- . Thus, from now on we describe the approximation method only for \mathbf{e}_+^a , since \mathbf{e}_-^a can be obtained directly by $-\mathbf{e}_+^a$. In this paper, the coefficients $\alpha_0, \alpha_1, \alpha_2, \alpha_3$ in (3.1) are determined such that \mathbf{e}_+^a is a G^2 Hermite interpolation of \mathbf{e}_+ . Accordingly, we show that the approximation $\mathbf{x} * \mathbf{e}_\pm^a$ is a G^2 Hermite interpolation of the offset curve $\mathbf{x} * \mathbf{e}_\pm$, respectively.

Since $\mathbf{e}_+^a(0) = \mathbf{e}_+(0)$ in (3.1), the curve \mathbf{e}_+^a is a G^0 Hermite interpolation of \mathbf{e}_+ if $\mathbf{e}_+^a(1) = \mathbf{e}_+(1)$ holds. The equation $\mathbf{e}_+^a(1) = \mathbf{e}_+(1)$ is equivalent to

$$\sum_{i=1}^2 \int_0^1 \mathbf{x}'(t) B_i^3(t) dt \alpha_i = (\mathbf{e}_+(1) - \mathbf{e}_+(0)) - \sum_{i=0}^1 \int_0^1 \mathbf{x}'(t) B_{3i}^3(t) dt \alpha_{3i}. \quad (3.2)$$

This is a linear equation with respect to α_1 and α_2 , i.e., (3.2) can be represented by

$$\mathbf{v}_1 \alpha_1 + \mathbf{v}_2 \alpha_2 = \mathbf{v},$$

where

$$\mathbf{v}_i = \int_0^1 \mathbf{x}'(t) B_i^3(t) dt, \quad i = 1, 2, \quad (3.3)$$

and \mathbf{v} denotes the right side of (3.2). The linear equation in (3.2) for α_1 and α_2 has a unique solution,

$$\alpha_1 = \frac{\mathbf{v} \times \mathbf{v}_2}{\mathbf{v}_1 \times \mathbf{v}_2}, \quad \alpha_2 = \frac{\mathbf{v}_1 \times \mathbf{v}}{\mathbf{v}_1 \times \mathbf{v}_2}, \quad (3.4)$$

if \mathbf{x} is convex and its Gauss map has a length less than π , where $(x_1, y_1) \times (x_2, y_2) = x_1 y_2 - x_2 y_1$.

From now on we assume that the regular parametric curve \mathbf{x} satisfies the sufficient condition for the existence of the solution of (3.2) uniquely: \mathbf{x} is convex and its Gauss map has a length less than π . If not, we can make \mathbf{x} satisfy the sufficient condition by subdividing \mathbf{x} at inflection points and repetitive bisections. Thus the curvature of \mathbf{x} is of constant sign in the domain interior. The approximation curve \mathbf{e}_+^a with α_1, α_2 satisfying (3.4) is a G^0 Hermite interpolation of \mathbf{e}_+ . Now, we find the two coefficients α_0, α_3 such that \mathbf{e}_+^a is a G^2 Hermite interpolation of \mathbf{e}_+ .

Proposition 3.1. *The two curves \mathbf{e}_+^a and \mathbf{e}_+ have the same curvature at both endpoints if and only if $|\alpha_{3i}| = \kappa_{\mathbf{x}}(i)/\kappa_{\mathbf{e}_+}(i)$, $i = 0, 1$.*

Proof. It follows from (3.1) that

$$\mathbf{e}_+^{a'}(i) = \alpha_{3i} \mathbf{x}'(i), \quad \mathbf{e}_+^{a''}(i) = \alpha_{3i}^2 \mathbf{x}''(i) + 3\Delta\alpha_{2i} \mathbf{x}'(i), \quad (3.5)$$

for $i = 0, 1$, where $\Delta\alpha_i = \alpha_{i+1} - \alpha_i$. Thus, we have

$$\mathbf{e}_+^{a'}(i) \times \mathbf{e}_+^{a''}(i) = \alpha_{3i}^2 \mathbf{x}'(i) \times \mathbf{x}''(i), \quad (3.6)$$

$i = 0, 1$, and

$$\kappa_{\mathbf{e}_+^a}(i) = \frac{\mathbf{e}_+^{a'}(i) \times \mathbf{e}_+^{a''}(i)}{\|\mathbf{e}_+^{a'}(i)\|^3} = \frac{\mathbf{x}'(i) \times \mathbf{x}''(i)}{|\alpha_{3i}| \|\mathbf{x}'(i)\|^3} = \frac{\kappa_{\mathbf{x}}(i)}{|\alpha_{3i}|}.$$

Hence, $\kappa_{\mathbf{e}_+^a}(i) = \kappa_{\mathbf{e}_+}(i)$, $i = 0, 1$, if and only if $\kappa_{\mathbf{x}}(i) = \kappa_{\mathbf{e}_+}(i)|\alpha_{3i}|$, and the assertion follows. \square

By the proposition above, we have two choices of $\alpha_{3i} = \kappa_{\mathbf{x}}(i)/\kappa_{\mathbf{e}_+}(i)$ or $-\kappa_{\mathbf{x}}(i)/\kappa_{\mathbf{e}_+}(i)$, $i = 0, 1$. Note that, in general, the sign of $\kappa_{\mathbf{x}}$ coincides with that of $\kappa_{\mathbf{e}_+}$. From (2.2) it follows that

$$\mathbf{e}'_+(i) = \pm \frac{\kappa_{\mathbf{x}}(i)}{\kappa_{\mathbf{e}_+}(i)} \mathbf{x}'(i), \quad (3.7)$$

where the + sign holds if \mathbf{x} is turning left and the – sign holds if \mathbf{x} is turning right. If \mathbf{x} is turning left, then it is parallel to \mathbf{e}_+ . We choose

$$\alpha_{3i} = \frac{\kappa_{\mathbf{x}}(i)}{\kappa_{\mathbf{e}_+}(i)}, \quad i = 0, 1, \quad (3.8)$$

so that

$$\mathbf{e}_+^{a'}(i) = \alpha_{3i} \mathbf{x}'(i) = \frac{\kappa_{\mathbf{x}}(i)}{\kappa_{\mathbf{e}_+}(i)} \mathbf{x}'(i) = \mathbf{e}'_+(i), \quad (3.9)$$

by (3.7). Reversely, if \mathbf{x} is turning right, then it is antiparallel to \mathbf{e}_+ . We choose

$$\alpha_{3i} = -\frac{\kappa_{\mathbf{x}}(i)}{\kappa_{\mathbf{e}_+}(i)}, \quad i = 0, 1, \quad (3.10)$$

so that

$$\mathbf{e}_+^{a'}(i) = \alpha_{3i} \mathbf{x}'(i) = -\frac{\kappa_{\mathbf{x}}(i)}{\kappa_{\mathbf{e}_+}(i)} \mathbf{x}'(i) = \mathbf{e}'_+(i), \quad (3.11)$$

by (3.7). With the choice of α_{3i} in (3.8) and (3.10), $i = 0, 1$, we show that the curve $\mathbf{x} * \mathbf{e}_+^a$ is a G^2 and C^1 Hermite interpolation of the offset curve $\mathbf{x} * \mathbf{e}_+$ as follows.

Proposition 3.2. *The approximant $\mathbf{x} * \mathbf{e}_+^a$ is a G^2 and C^1 Hermite interpolation of $\mathbf{x} * \mathbf{e}_+$.*

Proof. Since \mathbf{e}_+^a is at least a G^0 interpolation of \mathbf{e}_+ , we have $\mathbf{e}_+^a(i) = \mathbf{e}_+(i)$, $i = 0, 1$, and so, we obtain $(\mathbf{x} * \mathbf{e}_+^a)(i) = (\mathbf{x} * \mathbf{e}_+)(i)$. It follows from (3.9) and (3.11) that

$$\mathbf{e}_+^{a'}(i) = \mathbf{e}'_+(i), \quad i = 0, 1, \quad (3.12)$$

and that

$$(\mathbf{x} * \mathbf{e}_+^a)'(i) = (\mathbf{x} * \mathbf{e}_+)'(i), \quad i = 0, 1, \quad (3.13)$$

which implies that $\mathbf{x} * \mathbf{e}_+^a$ is a C^1 Hermite interpolation of $\mathbf{x} * \mathbf{e}_+$.

It is sufficient to show that $\kappa_{\mathbf{x} * \mathbf{e}_+^a}(i) = \kappa_{\mathbf{x} * \mathbf{e}_+}(i)$ for $i = 0, 1$. In the case of $\kappa_{\mathbf{x}}(i) \neq 0$, by Proposition 3.1, (3.8) and (3.10), we have $\kappa_{\mathbf{e}_+^a}(i) = \kappa_{\mathbf{e}_+}(i)$. It follows from (2.1) that

$$\kappa_{\mathbf{x} * \mathbf{e}_+^a}(i) = \kappa_{\mathbf{x} * \mathbf{e}_+}(i).$$

In the case of $\kappa_{\mathbf{x}}(i) = 0$, even if $\kappa_{\mathbf{e}_+^a}(i) \neq \kappa_{\mathbf{e}_+}(i)$, we have

$$\kappa_{\mathbf{x} * \mathbf{e}_+^a}(i) = 0 = \kappa_{\mathbf{x} * \mathbf{e}_+}(i),$$

by (2.1), since the curvature of the convolution curve is zero if at least one of the two curves is of curvature zero. Hence, the curvature of $\mathbf{x} * \mathbf{e}_+^a$ is equal to that of $\mathbf{x} * \mathbf{e}_+$ at both end points, and thus $\mathbf{x} * \mathbf{e}_+^a$ is the G^2 Hermite interpolation of $\mathbf{x} * \mathbf{e}_+$. \square

The approximant \mathbf{e}_-^a can be obtained by $\mathbf{e}_-^a = -\mathbf{e}_+^a$, and it is a G^2 and C^1 Hermite interpolation of \mathbf{e}_- for the same reason as in Proposition 3.2.

If \mathbf{e} is represented by

$$\mathbf{e}(s) = R_\theta(a \cos s, b \sin s)^T,$$

where R_θ is the rotation operator by the angle θ counterclockwise, then it is interesting that

$$\alpha_{3i} = \frac{\kappa_{\mathbf{x}}(i)}{\kappa_{\mathbf{e}}(s_+(i))}, \quad i = 0, 1, \quad (3.14)$$

whether \mathbf{x} is turning left or right, since $\kappa_{\mathbf{e}}(s_+(i)) = \kappa_{\mathbf{e}_+}(i)$ as \mathbf{x} is turning left, and $\kappa_{\mathbf{e}}(s_+(i)) = -\kappa_{\mathbf{e}_+}(i)$ as \mathbf{x} is turning right.

If \mathbf{x} is a regular polynomial curve, then our method yields a polynomial approximant of the convolution curve of \mathbf{x} and \mathbf{e} , which is a main merit of our method. Let $\mathbf{x} : [0, 1] \rightarrow \mathbb{R}^2$ be the parametric polynomial curve of degree n expressed in Bernstein-Bézier form as

$$\mathbf{x}(t) = \sum_{j=0}^n \mathbf{b}_j B_j^n(t),$$

where $\mathbf{b}_j, j = 0, 1, \dots, n$, are the control points of \mathbf{x} . It follows from (3.1) that \mathbf{e}_+^a is a polynomial curve of degree $n + 3$, and so is $\mathbf{x} * \mathbf{e}_+^a$. Equation (3.2) and the definition of \mathbf{v} yield

$$\begin{aligned} \mathbf{v}_i &= \frac{3n}{n+3} \sum_{j=0}^{n-1} \frac{\binom{n-1}{j}}{\binom{n+2}{i+j}} \Delta \mathbf{b}_j, \quad i = 1, 2, \\ \mathbf{v} &= \mathbf{e}_+(1) - \mathbf{e}_+(0) - \frac{n}{n+3} \sum_{j=0}^{n-1} \left(\frac{\alpha_0}{\binom{n+2}{j}} + \frac{\alpha_3}{\binom{n+2}{3+j}} \right) \binom{n-1}{j} \Delta \mathbf{b}_j. \end{aligned}$$

Thus, the coefficients α_1 and α_2 are obtained in the form of control points \mathbf{b}_j of \mathbf{x} by (3.4), and so are α_0 and α_3 by (3.14).

4. Approximation method and numerical examples

In this section, we describe our approximation method and apply it to numerical examples in the literature.

Our approximation method yields a curvature continuous polynomial spline curve of degree $n + 3$ approximating the convolution curve of the trajectory and ellipse when the trajectory is a polynomial curve of degree n . Our approximation method consists of a preprocess and a main process. In the preprocess, the trajectory curve \mathbf{x} is subdivided properly, and in the main subprocess, each convolution curve for the subdivided segment is approximated.

In the preprocess, the trajectory curve \mathbf{x} should be subdivided so that each subdivided segment becomes convex and the length of its Gauss map becomes less than π . If the Gauss map has a length larger than π , \mathbf{x} is subdivided into m pieces, where m is the smallest number such that the Gauss map of the subdivided piece is of length less than π . Then the cubic polynomial α exists uniquely by (3.4), (3.8), and (3.10). The Hausdorff distance between two curves, $\mathbf{x} * \mathbf{e}_\pm$ and $\mathbf{x} * \mathbf{e}_\pm^a$ is measured by

$$d_H(\mathbf{x} * \mathbf{e}_\pm, \mathbf{x} * \mathbf{e}_\pm^a) = d_H(\mathbf{e}_\pm, \mathbf{e}_\pm^a), \quad (4.1)$$

from (2.3), if these curves are regular. Thus, \mathbf{x} is subdivided at the point where $\mathbf{x} * \mathbf{e}_{\pm}$ has a cusp. Note that $\mathbf{x} * \mathbf{e}_{+}$ and $\mathbf{x} * \mathbf{e}_{-}$ can have cusps at different points in general. Thus, even for the same trajectory curve \mathbf{x} , the subdivision points for approximating $\mathbf{x} * \mathbf{e}_{+}$ and $\mathbf{x} * \mathbf{e}_{-}$ can be different. In the preprocess, \mathbf{x} is first subdivided at the inflection points and the points where $\mathbf{x} * \mathbf{e}_{+}$ or $\mathbf{x} * \mathbf{e}_{-}$ has cusps, and then \mathbf{x} is subdivided into a number of segments as small as possible if its Gauss map has a length larger than π .

In the main process, each convolution curve $\mathbf{x} * \mathbf{e}_{\pm}$ of the subdivided segment and corresponding ellipse segment is approximated by the approximant $\mathbf{x} * \mathbf{e}_{\pm}^a$ using the divide-and-conquer method. If the error is larger than the given tolerance, then the segment is subdivided into two segments, and then they are approximated separately. This process is repeated until the error is less than the tolerance.

We consider two numerical examples which were presented in previous works [17, 21]. The first example is the convolution approximation of a cubic spline and an ellipse [17]. The trajectory curve is a cubic spline composed of five cubic Bézier curves and is C^2 continuous except for one cusp, as shown in Figure 1. The ellipse is parameterized by $\mathbf{e}(s) = R_{\pi/6}(\cos s, 0.3 \sin s)^T$. The cubic spline is subdivided into five Bézier curves, and none of them has an inflection point. In order to use (4.1), we find the cusp of $\mathbf{x} * \mathbf{e}_{\pm}$. Since the cubic spline \mathbf{x} is turning right, the convolution curve $\mathbf{x} * \mathbf{e}_{-}$ does not have a cusp, and $\mathbf{x} * \mathbf{e}_{+}$ has four cusps, where \mathbf{x} is subdivided for approximating $\mathbf{x} * \mathbf{e}_{+}$, as shown in Figure 1. The lengths of the Gauss map of the former four Bézier curves are less than π , but that of the last Bézier curve is larger than π , and so a subdivision is needed for approximating $\mathbf{x} * \mathbf{e}_{-}$. Thus, in the preprocess, \mathbf{x} is subdivided into nine and six segments for approximating $\mathbf{x} * \mathbf{e}_{+}$ and $\mathbf{x} * \mathbf{e}_{-}$, respectively. Our method yields the spline approximant of degree six, since the trajectory curve is a cubic spline. For $TOL = 10^{-1}$, the minimal numbers of segments of hexic polynomial curves approximating the convolution curves $\mathbf{x} * \mathbf{e}_{+}$ and $\mathbf{x} * \mathbf{e}_{-}$ with the error less than TOL are nine and seven, respectively, as shown in Figure 1. We can see that the minimum numbers of segments of hexic approximants approximating $\mathbf{x} * \mathbf{e}_{+}$ are larger than those approximating $\mathbf{x} * \mathbf{e}_{-}$, since $\mathbf{x} * \mathbf{e}_{+}$ has a higher number of cusps than $\mathbf{x} * \mathbf{e}_{-}$. For each tolerance, the minimum number of segments of hexic approximants with the error less than the tolerance can be obtained as in Table 1. We implement the approximation method presented in [17] and add the results from the method in Table 1. With respect to the minimum number of segments of approximants, the method in [17] requires smaller numbers of segments than our method. However, our method yields a polynomial approximant, and its degree is six, whereas the method in [17] obtains a rational approximant whose degree is eleven.

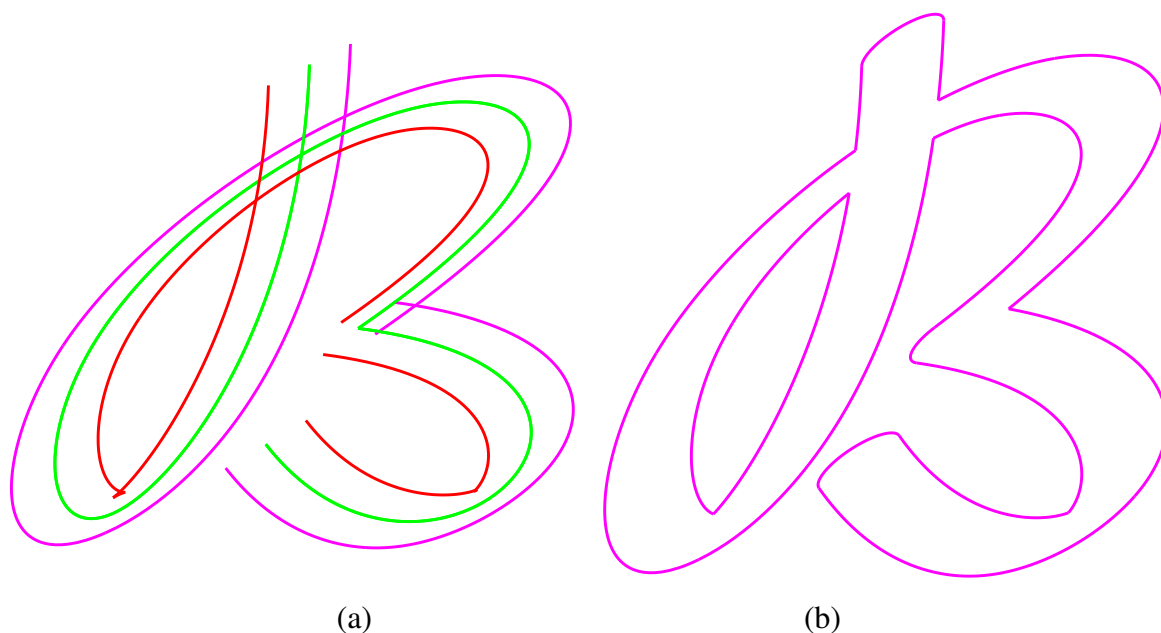


Figure 1. (a) Hexic G^2 polynomial curves $\mathbf{x} * \mathbf{e}_+^a$ (red color) and $\mathbf{x} * \mathbf{e}_-^a$ (magenta) approximating the convolution curves $\mathbf{x} * \mathbf{e}_+$ and $\mathbf{x} * \mathbf{e}_-$, respectively, of the cubic spline \mathbf{x} (green) and an ellipse. They are constructed by 13 and 11 segments, respectively, and their errors are less than 10^{-2} ; (b) Trimmed curves of $\mathbf{x} * \mathbf{e}_+^a$ and $\mathbf{x} * \mathbf{e}_-^a$ and three closures, which are hexic polynomial curves approximating the half ellipses or a smaller part of the ellipse.

Table 1. Minimum number of segments of approximation curves using the method in [17] and our method, respectively, needed for approximating the convolution curves in Figure 1, with errors less than TOL .

TOL	[17]	Our method	TOL	[17]	Our method
10^{-1}	9	9	10^{-1}	6	7
10^{-2}	11	13	10^{-2}	11	11
10^{-3}	14	17	10^{-3}	12	18
10^{-4}	18	24	10^{-4}	18	24
10^{-5}	27	35	10^{-5}	25	33

(a) Right boundary $\mathbf{x} * \mathbf{e}_+$.

(b) Left boundary $\mathbf{x} * \mathbf{e}_-$.

The second example is the approximation of the convolution curve of a nonic Bézier curve and an ellipse [21, 22]. Our method yields the curvature continuous polynomial curve of degree twelve approximating the convolution curve. The nonic Bézier curve \mathbf{x} has one inflection point, and its convolution curves $\mathbf{x} * \mathbf{e}_+$ and $\mathbf{x} * \mathbf{e}_-$ have two and four cusps, respectively, as shown in Figure 2. The trajectory curve is subdivided at the inflection point and at the point where the convolution curve has cusp, and is also subdivided so that its Gauss map is of length less than π in the preprocess. Thus, \mathbf{x} is subdivided into six and seven segments for approximating $\mathbf{x} * \mathbf{e}_+$ and $\mathbf{x} * \mathbf{e}_-$, respectively. In the main process each subdivided segment is approximated and subdivided repeatedly until the error is less than the given tolerance. For each tolerance, the minimum number of segments of approximants with the

error less than the tolerance is listed in Table 2. We implement the approximation method presented in [12] and obtain the results using the method. The minimum numbers of segments achieved by our method are much smaller than those obtained by the method in [12], as shown in Table 2. Moreover, our method yields G^2 Hermite interpolation, whereas the method in [12] obtains only G^1 Hermite interpolation. However, the degree of the approximation curve obtained by the method in [12] is three, which is smaller than that achieved by our method. The approximant is of degree twelve, since \mathbf{x} in this example is of degree nine.

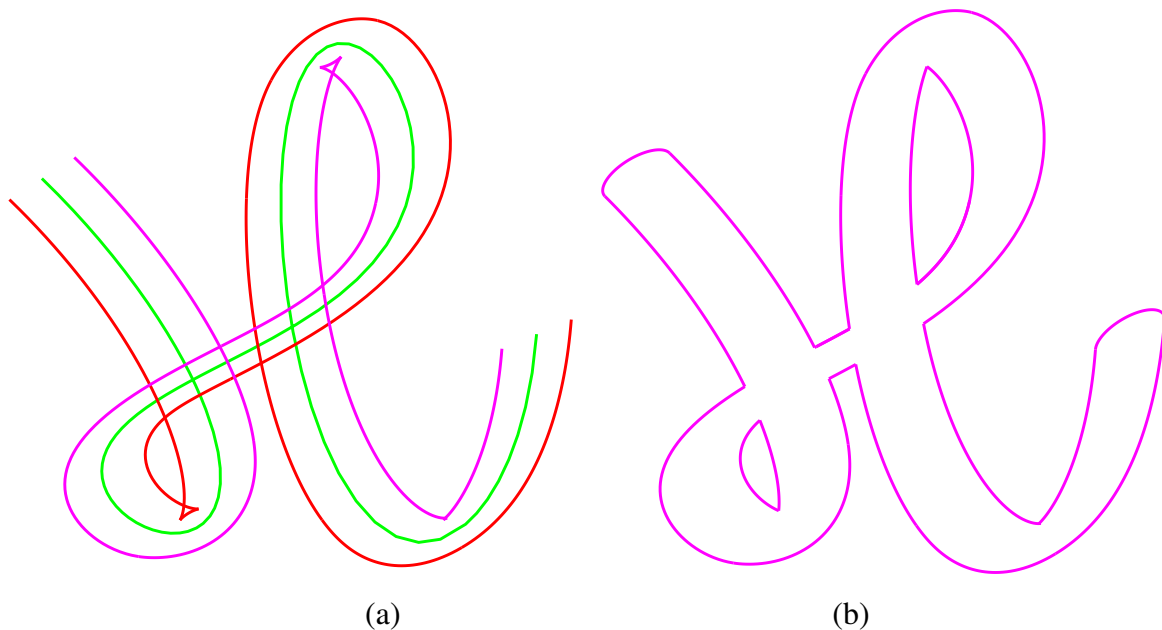


Figure 2. (a) G^2 polynomial curves $\mathbf{x} * \mathbf{e}_+^a$ (red color) and $\mathbf{x} * \mathbf{e}_-^a$ (magenta) of degree twelve approximating the convolution curves $\mathbf{x} * \mathbf{e}_+$ and $\mathbf{x} * \mathbf{e}_-$, respectively, of a nonic Bézier curve \mathbf{x} (green) and an ellipse. They are constructed by 13 and 11 segments, respectively, and their errors are less than 10^{-2} ; (b) Trimmed curves of $\mathbf{x} * \mathbf{e}_+^a$ and $\mathbf{x} * \mathbf{e}_-^a$ and two closures, which are polynomial curves of degree twelve approximating the half ellipses.

Table 2. Minimum number of segments of approximation curves using the method in [12] and our method, respectively, needed for approximating the convolution curves in Figure 2, with errors less than TOL .

TOL	[12]	Our method	TOL	[12]	Our method
10^{-1}	13	9	10^{-1}	14	10
10^{-2}	24	15	10^{-2}	25	15
10^{-3}	42	25	10^{-3}	43	24
10^{-4}	77	31	10^{-4}	79	34
10^{-5}	141	49	10^{-5}	143	47

(a) Right boundary $\mathbf{x} * \mathbf{e}_+$. (b) Left boundary $\mathbf{x} * \mathbf{e}_-$.

As shown in Figure 1, the approximant $\mathbf{x} * \mathbf{e}_+^a$ has two self-loops, and $\mathbf{x} * \mathbf{e}_-^a$ has one self-intersection

point. The trimmed curve can be obtained by removing the self-loops and the redundant segments near the self-intersection point. In order to complete the construction of the font, three closures are needed. The closures are half ellipses or a smaller part of the ellipse, which are approximated by hexic polynomial curves. Applying the approximation method of circular arcs by hexic polynomial curves [23], we obtained the approximants with an error less than 2.683×10^{-7} , as shown in Figure 1(b). As shown in Figure 2, $\mathbf{x} + \mathbf{e}_+^a$ and $\mathbf{x} + \mathbf{e}_-^a$ have one and two self-loops, respectively. The construction of the font can be completed by trimming the loops and adding two closures. The closures are half ellipses and are approximated by polynomial curves of degree twelve. After the half ellipses are approximated by Bézier curves of degree eleven using the half ellipse approximation method [24, 25], the approximant can be expressed in Bézier form of degree twelve by the degree elevation [26]. The error for approximating the half ellipse is 5.963×10^{-6} , as shown in Figure 2(b).

5. Conclusions

In this paper, we presented the convolution approximation method for regular plane parametric curves and ellipses. Our method yields the G^2 and C^1 Hermite interpolation of the convolution curve, and yields a polynomial approximant for the convolution curve whenever the trajectory curve is a polynomial curve. We compared the numerical results of our method with those of previous methods, and analyzed the merits of our method. Compared with previous methods, the merits of our method are that the approximant is a G^2 and C^1 Hermite interpolation, and the degree of the approximant or the required number of segments of the approximant within error tolerances is small.

Acknowledgements

This study was supported by research funds from Chosun University, 2023, and by Basic Science Research Program through the National Research Foundation of Korea (NRF) funded by the Ministry of Education (NRF-2021R1F1A1045830). The author is very grateful to three anonymous reviewers for their valuable comments and constructive suggestions.

Conflict of interest

The author declares no conflict of interest.

References

1. I.-K. Lee, M.-S. Kim, G. Elber, Polynomial/rational approximation of Minkowski sum boundary curves, *Graphical Models and Image Processing*, **60** (1998), 136–165. <https://doi.org/10.1006/gmip.1998.0464>
2. R. Yamada, T. Tsuji, T. Hiramitsu, H. Seki, T. Nishimura, Y. Suzuki, et al., Fast and precise approximation of minkowski sum of two rotational ellipsoids with a superellipsoid, *Vis. Comput.*, **40** (2024), 4609–4621. <https://doi.org/10.1007/s00371-024-03445-9>
3. C. L. Bajaj, M.-S. Kim, Generation of configuration space obstacles: The case of moving algebraic curves, *Algorithmica*, **4** (1989), 157–172. <https://doi.org/10.1007/BF01553884>

4. M. Kohler, M. Spreng, Fast computation of the C-space of convex 2D algebraic objects, *Int. J. Robot. Res.*, **14** (1995), 590–608. <https://doi.org/10.1177/027836499501400605>
5. S. Ruan, G. S. Chirikjian, Closed-form Minkowski sums of convex bodies with smooth positively curved boundaries, *Comput.-Aided Design*, **143** (2022), 103133. <https://doi.org/10.1016/j.cad.2021.103133>
6. J. Vršek, M. Lávička, On convolutions of algebraic curves, *J. Symb. Comput.*, **45** (2010), 657–676. <https://doi.org/10.1016/j.jsc.2010.02.001>
7. J. Vršek, M. Lávička, Exploring hypersurfaces with offset-like convolutions, *Comput. Aided Geom. D.*, **29** (2012), 676–690. <https://doi.org/10.1016/j.cagd.2012.07.002>
8. Y. J. Ahn, C. Hoffmann, Y. S. Kim, Curvature-continuous offset approximation based on circle approximation using quadratic Bézier biarcs, *Comput.-Aided Design*, **43** (2011), 1011–1017. <https://doi.org/10.1016/j.cad.2011.04.005>
9. R. Lee, Y. J. Ahn, Geometric shape analysis for convolution curve of two compatible quadratic Bézier curves, *J. Comput. Appl. Math.*, **288** (2015), 141–150. <https://doi.org/10.1016/j.cam.2015.04.012>
10. I.-K. Lee, M.-S. Kim, G. Elber, Planar curve offset based on circle approximation, *Comput.-Aided Design*, **28** (1996), 617–630. [https://doi.org/10.1016/0010-4485\(95\)00078-X](https://doi.org/10.1016/0010-4485(95)00078-X)
11. S. W. Kim, S. C. Bae, Y. J. Ahn, An algorithm for G^2 offset approximation based on circle approximation by G^2 quadratic spline, *Comput.-Aided Design*, **73** (2016), 36–40. <https://doi.org/10.1016/j.cad.2015.11.003>
12. Y. J. Ahn, C. M. Hoffmann, Approximate convolution with pairs of cubic Bézier LN curves, *Comput. Aided Geom. D.*, **28** (2011), 357–367. <https://doi.org/10.1016/j.cagd.2011.06.006>
13. B. Jüttler, Triangular Bézier surface patches with a linear normal vector field, In: *The mathematics of surfaces VIII, information geometers*, Winchester, 1998, 431–446.
14. B. Jüttler, M. L. Sampoli, Hermite interpolation by piecewise polynomial surfaces with rational offsets, *Comput. Aided Geom. D.*, **17** (2000), 361–385. [https://doi.org/10.1016/S0167-8396\(00\)00002-9](https://doi.org/10.1016/S0167-8396(00)00002-9)
15. M. L. Sampoli, Computing the convolution and the Minkowski sum of surfaces, *Proceedings of the 21st Spring Conference on Computer Graphics*, New York: Association for Computing Machinery, 2005, 111–117. <https://doi.org/10.1145/1090122.1090142>
16. M. L. Sampoli, M. Peternell, B. Jüttler, Rational surfaces with linear normals and their convolutions with rational surfaces, *Comput. Aided Geom. D.*, **23** (2006), 179–192. <https://doi.org/10.1016/j.cagd.2005.07.001>
17. Y. J. Ahn, C. Hoffmann, Sequence of G^n LN polynomial curves approximating circular arcs, *J. Comput. Appl. Math.*, **341** (2018), 117–126. <https://doi.org/10.1016/j.cam.2018.03.028>
18. R. T. Farouki, H. P. Moon, B. Ravani, Algorithms for Minkowski products and implicitly-defined complex sets, *Adv. Comput. Math.*, **13** (2000), 199–229. <https://doi.org/10.1023/A:1018910412112>

19. S. W. Kim, R. Lee, Y. J. Ahn, A new method approximating offset curve by Bézier curve using parallel derivative curves, *Comp. Appl. Math.*, **37** (2018), 2053–2064. <https://doi.org/10.1007/s40314-017-0437-x>
20. Y. J. Ahn, G^2/C^1 Hermite interpolation of offset curves of parametric regular curves, *AIMS Mathematics*, **8** (2023), 31008–31021. <https://doi.org/10.3934/math.20231587>
21. Y. J. Ahn, C. Hoffmann, Circle approximation using LN Bézier curves of even degree and its application, *J. Math. Anal. Appl.*, **410** (2014), 257–266. <https://doi.org/10.1016/j.jmaa.2013.07.079>
22. Y. J. Ahn, J. Cui, C. Hoffmann, Circle approximations on spheroids, *J. Navigation*, **64** (2011), 739–749. <https://doi.org/10.1017/S0373463311000294>
23. H. M. Yoon, Y. J. Ahn, Circular arc approximation by hexic polynomial curves, *Comp. Appl. Math.*, **42** (2023), 265. <https://doi.org/10.1007/s40314-023-02315-9>
24. M. Floater, An $O(h^{2n})$ Hermite approximation for conic sections, *Comput. Aided Geom. D.*, **14** (1997), 135–151. [https://doi.org/10.1016/S0167-8396\(96\)00025-8](https://doi.org/10.1016/S0167-8396(96)00025-8)
25. Y. J. Ahn, A property of parametric polynomial approximants of half circles, *Comput. Aided Geom. D.*, **87** (2021), 101990. <https://doi.org/10.1016/j.cagd.2021.101990>
26. B.-G. Lee, Y. Park, J. Yoo, Application of Legendre-Bernstein basis transformations to degree elevation and degree reduction, *Comput. Aided Geom. D.*, **19** (2002), 709–718. [https://doi.org/10.1016/S0167-8396\(02\)00164-4](https://doi.org/10.1016/S0167-8396(02)00164-4)



AIMS Press

©2024 the Author(s), licensee AIMS Press. This is an open access article distributed under the terms of the Creative Commons Attribution License (<https://creativecommons.org/licenses/by/4.0>)